

Ray-Tracing vs. 3GPP TDL: Power Delay Profile Analysis in Outdoor-to-Indoor and Indoor Channels

Julia Andrusenko
Rampart Communications
Linthicum Heights, MD
USA

jandrusenko@rampartcommunications.com

Chloe Makdad
Rampart Communications
Linthicum Heights, MD
USA

cmakdad@rampartcommunications.com

Abstract—3rd Generation Partnership Project (3GPP) Technical Report (TR) 38.901 channel models (Releases 15-19) are widely used for physical-layer design and system-level evaluation in dense urban outdoor-to-indoor (O2I) and indoor environments. These models capture ensemble-averaged channel statistics but do not account for site-specific geometry. In this paper, we compare Power Delay Profiles (PDPs) derived from a deterministic ray-tracing model (Remcom Wireless InSite software) with those from the 3GPP TR 38.901 Tapped Delay Line (TDL) channel models. This comparative analysis is performed using a dense urban O2I scenario and a representative single-story indoor layout modeled in Washington, D.C., under matched link-distance and Non-Line-of-Sight (NLOS) conditions. All Wireless InSite PDPs are power-normalized to enable comparison of relative multipath delay structure.

We evaluate root-mean-square (RMS) delay spread, mean excess delay, effective maximum delay, and Kullback-Leibler (KL) distribution divergence. Results indicate that 3GPP TDL models generally exhibit longer delay spreads and often fail to capture deterministic, site-specific features such as late-arriving energy and irregular spikes. While TDL models can approximate primary channel features in some cases, their reliance on ensemble-averaged statistics rather than geometry limits their representation of fine multipath structures. We conclude that while 3GPP TDL models are suitable for large-scale system evaluation, deterministic or hybrid approaches are more appropriate for site-specific physical-layer design.

Index Terms—3GPP, tapped delay line, power delay profile, ray tracing, stochastic channel models, deterministic channel modeling, outdoor-to-indoor, indoor propagation, non-line-of-sight, delay spread, 5G, multipath.

I. INTRODUCTION

THE 3rd Generation Partnership Project (3GPP) Technical Report (TR) 38.901 [1] channel models are widely used for physical-layer design and system-level evaluation in dense urban outdoor-to-indoor (O2I) and indoor environments. These stochastic Tapped Delay Line (TDL) and Clustered Delay Line (CDL) models are statistically calibrated to measurement data and are designed to reproduce ensemble-average channel behavior across standardized deployment

scenarios. Related geometry-based stochastic models, including WINNER II [2] and COST 2100 [3], similarly reproduce spatial and statistical channel behavior using stochastic cluster evolution and spatial consistency mechanisms. However, these models do not explicitly account for site-specific geometry, street topology, or precise material properties, limiting their ability to capture deterministic multipath structure in a particular physical environment. In contrast, deterministic ray-tracing approaches model propagation directly from environmental geometry and electromagnetic material properties. Prior work has shown that deterministic ray-tracing methods can accurately reproduce measured Power Delay Profiles (PDPs), path loss, and delay spread characteristics in dense urban and indoor environments when detailed environmental geometry and material properties are available [4], [5], [6]. These differences raise questions regarding how accurately generic stochastic TDL profiles represent the complex multipath structure observed in a real urban or indoor environment.

This paper compares PDPs generated using the Remcom Wireless InSite deterministic ray-tracing platform [7] at a carrier frequency of 3.5 GHz against the 3GPP TR 38.901 TDL-A, TDL-B, and TDL-C Non-Line-of-Sight (NLOS) channel models. The study models a 1 km \times 1 km dense urban area in Washington, DC (Dupont Circle), featuring building construction materials with defined electrical properties, including concrete, asphalt, glass, and drywall. The propagation scenario includes two outdoor transmitters at 10 m height and one indoor transmitter at 1.5 m height, with a uniformly spaced 2-m receiver grid consisting of 666 first-floor receivers positioned at 1.5 m height. We did not have architectural blueprints, so a representative floorplan was replicated across all eight floors of a key building in the environment. The receiver grid was placed on the first floor of this representative building. We then selected a subset of receiver locations for which the ray-tracing simulation indicated link closure, and used the corresponding PDPs for detailed analysis.

We normalized selected Wireless InSite PDPs to the peak tap to remove link budget effects and enable comparison of the relative power distribution over delay. We then evaluated root-mean-square (RMS) delay spread, mean excess delay, effective maximum delay, and distribution divergence. For the Wireless InSite software predictions, a power threshold

This research was supported by the U.S. Department of Commerce's National Telecommunications and Information Administration (NTIA) under the Public Wireless Supply Chain Innovation Fund Grant Program (Award 24-60-IF2415: ASPEN - Advanced Signal Processing Enhancement for Next-Generation Open Radio Units), administered by the National Institute of Standards and Technology.

of -30 dB relative to the peak tap was applied when computing PDP statistics, including effective maximum delay. We selected a -30 dB threshold based on the smallest relative power level observed across the TDL-A, TDL-B, and TDL-C models. This thresholding reflects the fact that standardized 3GPP TDL models are statistical abstractions that do not preserve ultra-weak deterministic delay tails. While prior comparisons between stochastic and deterministic channel models often focus on scalar metrics such as path loss and RMS delay spread, fewer studies quantify full PDP structural differences using higher-order metrics. To address this limitation, this work utilizes Kullback–Leibler distribution divergence to explicitly quantify geometry-induced channel variance not captured by standardized stochastic channel models.

These results provide insights for physical-layer design, showing that while stochastic TDL models are suitable for ensemble-average performance evaluation, deterministic or hybrid geometry-aware models better capture site-specific multipath structure and delay-domain variability in dense urban and indoor environments. These differences are particularly relevant for system design considerations such as delay spread characterization and potential implications for inter-symbol interference (ISI) sensitivity and cyclic prefix dimensioning.

II. CHANNEL MODELING FRAMEWORK

A. Wireless InSite Model

To generate site-specific power delay profiles (PDPs), we used the Remcom Wireless InSite X3D shooting-and-bouncing-ray (SBR) propagation model with GPU acceleration, multithreading, and exact path calculations. The model accounts for terrain, structures, and building floorplans. Our prior studies have extensively validated this tool against measured wireless channel data. For example, in scattering-rich urban environments, predicted path loss achieved root mean square error (RMSE) values between 6.58 dB and 13.86 dB when compared against field measurements, which falls within the approximate 12–15 dB best-case RMSE range commonly reported for practical path loss models in the literature [8].

The modeled scenario consisted of a $1 \text{ km} \times 1 \text{ km}$ representation of the Dupont Circle area in Washington, D.C., including dense urban outdoor-to-indoor (O2I) and indoor-to-indoor (I2I) propagation conditions. Fig. 1 depicts the modeled Dupont Circle area, illustrating terrain and building height variability through color mapping, with the tallest building reaching approximately 48 m in height.

Fig. 2 depicts the Wireless InSite scenario layout, including two outdoor transmitters, one indoor transmitter, and a grid of 666 indoor receivers distributed across the first floor of a representative eight-story building. Although the building structure contains eight floors, only the first floor containing the receiver grid is shown for visualization clarity.

Wireless InSite X3D predicts multiple propagation metrics, including path loss, received power, time of arrival (TOA),

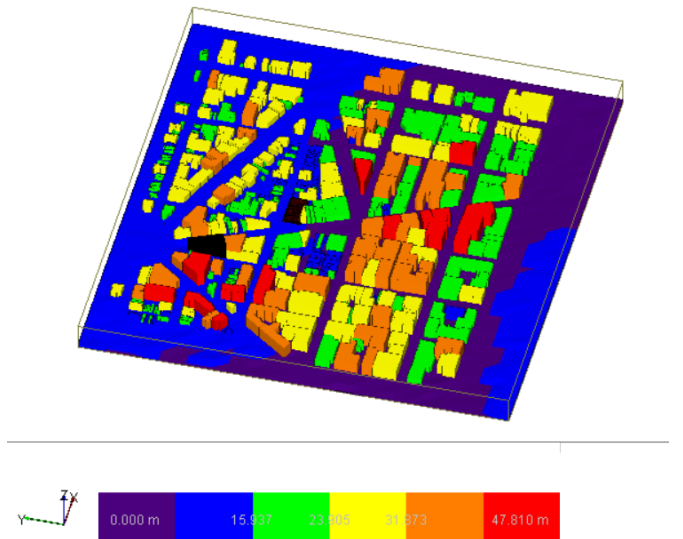


Fig. 1. Wireless InSite X3D model of the Dupont Circle scenario showing terrain and building height variability through color mapping. The tallest building in the modeled environment is approximately 48 m in height.



Fig. 2. Wireless InSite scenario layout showing two outdoor transmitters, one indoor transmitter, and a grid of 666 indoor receivers distributed across the first floor of a representative eight-story building.

time of departure (TOD), and complex impulse response. In this work, we focused specifically on the complex impulse response outputs that include absolute received powers, phases, and TOAs for each propagation path. These outputs were subsequently converted into power-normalized PDPs using excess delay rather than absolute TOA. Table I summarizes the primary modeling assumptions and simulation parameters used to generate the site-specific PDPs.

B. Processing Consistency and Thresholding

We normalized Wireless InSite PDPs to the peak tap to remove link budget effects and enable comparison of relative delay-domain power distributions. We then applied a -30 dB

TABLE I
WIRELESS INSITE MODELING PARAMETERS AND ASSUMPTIONS

Parameter	Value
Frequency	3.5 GHz
Propagation Model	Wireless InSite X3D SBR model
Environment	1 km × 1 km Dupont Circle dense urban and indoor scenario for O2I and indoor-to-indoor (I2I) propagation modeling
Outdoor Transmitters (O2I Tx1 and O2I Tx2)	10 m above ground level (AGL), below rooftop level; 0 dBi omnidirectional antennas
Indoor Transmitter (I2I Tx)	1.5 m AGL with a 0 dBi omnidirectional antenna
Receiver (Rx) Grid	666 indoor receivers distributed across the first floor at 1.5 m AGL with uniform 2 m spacing
Approximate Transmitter–Receiver Separation Distances	O2I Tx1 to Rx grid center: 66 m O2I Tx2 to Rx grid center: 70 m I2I Tx to Rx grid center: 8 m
Terrain Material	Asphalt: conductivity = 5.000×10^{-4} S/m, relative permittivity = 5.72
Building Materials	Concrete: conductivity = 0.123087 S/m, relative permittivity = 5.24, thickness = 0.3 m Glass: conductivity = 0.019276 S/m, relative permittivity = 6.31, thickness = 0.003 m Two-layer drywall: conductivity = 0.027579 S/m, relative permittivity = 2.73, thickness = 0.013 m
Representative Building	Eight-story building composed of concrete, glass, and drywall materials
Transmit Power	Outdoor transmitters: 5 W (41 dBm) Indoor transmitter: 3.16 W (35 dBm) Representative transmit power levels were selected to ensure link closure for PDP generation.

threshold relative to the peak tap, removing weak multipath components prior to metric computations.

We computed RMS delay spread, mean excess delay, effective maximum delay, and distribution divergence on the thresholded PDPs. We selected the -30 dB threshold based on the minimum relative power levels observed across the TDL-A, TDL-B, and TDL-C models.

This approach reflected that standardized 3GPP TDL models are statistical abstractions that do not retain ultra-weak deterministic delay tails.

C. Multipath Representation Implications

Multipath propagation introduces critical channel impairments such as delay spread, ISI, and frequency-selective fading. The severity of these impairments directly influences system design considerations including equalization complexity and cyclic prefix sizing. Deterministic ray-traced channels can exhibit irregular delay spreads, clustered multipath behavior, and strong geometry dependence, all of which influence coherence bandwidth, ISI severity, and synchronization sensitivity. In contrast, standardized TDL models employ fixed tap structures intended to reproduce average channel behavior, which can smooth or omit fine multipath characteristics and late-arriving energy components. In addition, the

TABLE II
TDL CHANNEL MODELS VS. WIRELESS INSITE X3D MODEL

Feature	TDL Models	Wireless InSite
Modeling basis	Statistical model from measurements	Geometry- and physics-based propagation
Multipath structure	Fixed tap delays and powers	Explicit path-resolved components
Delay spread	Ensemble-average behavior	Geometry-dependent behavior
ISI characteristics	May miss worst-case symbol overlap	Can exhibit severe ISI from geometry-dependent multipath
Frequency selectivity	Averaged fading response	Site-specific fading response
Tail energy	Limited late-arriving energy	Preserves late multipath energy
Spatial dependence	Weak geometry dependence	Strong geometry dependence
Synchronization sensitivity	Smoothed timing behavior	Geometry-driven timing variation
Equalization impact	Simplified impulse response (statistical average); predictable convergence behavior	Site-specific impulse response; geometry-dependent convergence and ISI behavior
Computational cost	Low	High
Representative application	System-level evaluation	Site-specific PHY analysis

TDL models are averaged over multiple channel realizations and employ fixed tap delays and relative tap powers across different delay spread regimes. However, the standard does not define a unique mapping between real environments and a specific TDL profile, so selection is based on approximate delay spread matching rather than geometry, further limiting the representation of fine multipath structure. Consequently, comparison between these modeling approaches is important, since simplified multipath representations may underestimate geometry-driven effects, particularly metrics related to tail energy and distribution divergence that are relevant to worst-case ISI assessment, cyclic prefix sizing, and site-specific physical-layer design. Table II summarizes the key differences between stochastic TDL models and deterministic Wireless InSite X3D ray-tracing model.

III. RESULTS

We now compare the PDPs of two O2I urban microcell (UMi) scenarios and one I2I scenario with each of the 3GPP NLOS TDL models. For each scenario, we evaluate five different receivers. Table III summarizes the delay metrics for the TDL models [1]. The RMS delay spread value (RMS) reflects the desired delay spread ($DS_{desired}$) parameter from the 3GPP standard, which is then used to compute mean excess delay (Mean) and effective maximum delay (Max), all presented in nanoseconds (ns). In Table IV, Table V, and Table VI, we consider five receivers (RX ID) per scenario and display the same metrics along with KL divergence, with the site-specific models used as the reference distribution. Both the TDL and site-specific PDPs are linearized, normalized

and interpolated before computing the KL divergence (D_{KL}) in bits.

The delay spreads from the 3GPP TDL models tend to have longer tails than our site-specific models. Comparing the O2I UMi scenarios from Table III to Table IV and Table V, we see that the RMS delay spread, mean excess delay, and max excess delay for the 3GPP models is always longer than our site-specific ones. When looking at the I2I scenarios in Table III and Table VI, the RMS delay spread, mean excess delay, and maximum excess delay for the 3GPP models is often longer than in the site-specific ones, though this is not always the case. Figure 3 and Figure 4 visualize this phenomenon for O2I Tx1 receiver 564 and I2I Tx receiver 32, respectively.

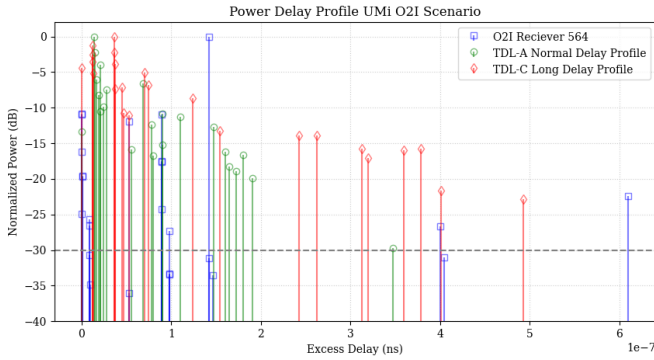


Fig. 3. Power delay profiles for receiver 564 from O2I Tx1, TDL-A UMi, and TDL-C UMi.

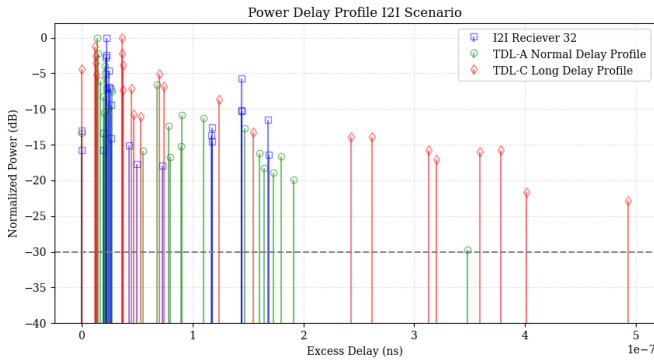


Fig. 4. Power delay profiles for receiver 32 from I2I Tx, TDL-A Indoor, and TDL-C Indoor.

TABLE III
3GPP TDL MODELS

Scenario	3GPP Model		Delays (ns)		
	TDL	Delay Profile	RMS	Mean	Max
UMi O2I	A	Normal	240	606.76	2000
I2I	A	Normal	36	91.013	347.71
UMi O2I	B	Normal	240	356.87	1000
I2I	B	Normal	36	53.530	172.20
UMi O2I	C	Long	616	2000	5000
I2I	C	Long	57	147.35	493.18

TABLE IV
WIRELESS INSITE OUTDOOR-TO-INDOOR 1

RX ID	Delays (ns)			KL Divergence (bits)		
	RMS	Mean	Max	TDL-A	TDL-B	TDL-C
489	64.654	87.078	610.23	2.8673	3.0893	0.84652
534	39.775	73.979	346.74	1.5593	0.71729	0.89663
564	62.443	98.888	610.21	2.6485	2.8273	3.3041
594	64.323	145.89	609.82	1.5414	0.94833	1.3592
602	43.571	35.989	89.714	1.4708	0.48239	0.67291

TABLE V
WIRELESS INSITE OUTDOOR-TO-INDOOR 2

RX ID	Delays (ns)			KL Divergence (bits)		
	RMS	Mean	Max	TDL-A	TDL-B	TDL-C
484	56.532	90.464	335.06	0.58889	0.59527	0.34415
521	81.067	92.487	334.85	0.57561	0.61502	0.35294
559	80.923	95.142	334.84	0.55559	0.56111	0.32814
595	45.762	87.650	335.72	0.64181	0.57692	0.46699
631	44.716	89.606	335.70	0.83714	0.55084	0.61937

For an approximating probability distribution Q and true probability distribution P , KL divergence

$$D_{KL}(P \parallel Q) = \sum_{x \in \mathcal{X}} P(x) \log_2 \left(\frac{P(x)}{Q(x)} \right)$$

is a measure of how much Q differs from P [9]. KL divergence can be used to model how well an approximate distribution fits a true distribution and has previously been used to evaluate channel models versus specific communication environments [10]. In this context, we evaluate how well the 3GPP TDL models approximate our site-specific PDPs. A KL divergence of 0 bits would mean that the 3GPP model is a perfect representation of the site-specific model, and higher KL divergence corresponds to more significant differences. Since we have computed KL divergence in terms of bits, we can interpret a $D_{KL} = 1$ as meaning that we would need one bit more per sample to represent the site-specific model with the 3GPP model than if we had simply used the site-specific model. Computing KL divergence requires us to normalize the power delay profiles, so the metric does not reflect differences in delay spread.

The data show many scenarios with notable differences between the 3GPP TDL models and our site-specific PDPs, particularly in our first O2I scenario and our I2I scenario. Receiver 564 in Table IV and receiver 36 in Table VI each show massive differences with all three TDL models. Figure 7 shows the normalized PDP for receiver 564 versus the

TABLE VI
WIRELESS INSITE INDOOR-TO-INDOOR

RX ID	Delays (ns)			KL Divergence (bits)		
	RMS	Mean	Max	TDL-A	TDL-B	TDL-C
32	43.930	62.649	168.84	1.1602	1.9451	0.61730
36	12.796	39.642	148.07	2.7942	2.9244	2.0677
69	18.262	32.789	97.297	0.80462	1.0688	0.59745
176	28.131	126.85	164.45	1.7332	1.0914	1.6052
259	23.507	39.642	104.02	2.7493	0.89891	1.7138

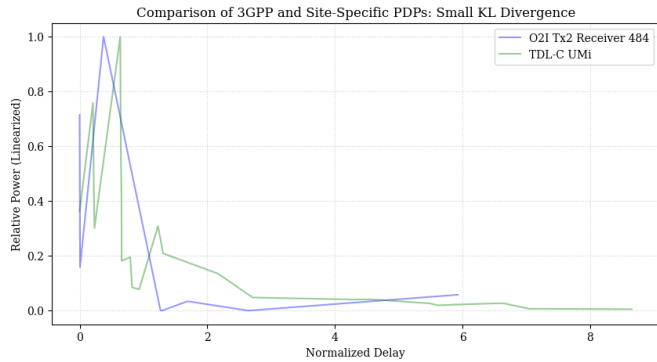


Fig. 5. A comparison of the normalized PDPs of 3GPP TDL-C UMi and receiver 484 from the O2I Tx2. The KL Divergence of these PDPs is small, and the 3GPP model reflects the main features of the site-specific model.

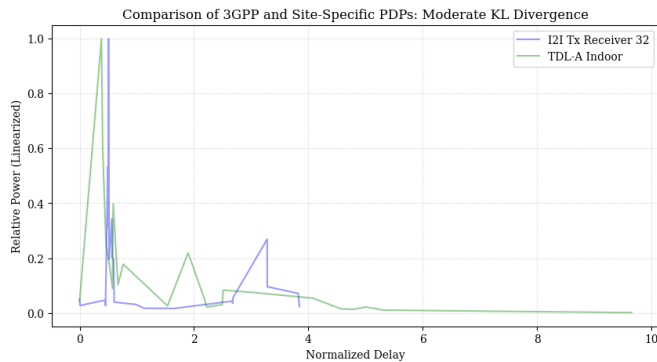


Fig. 6. A comparison of the normalized PDPs of 3GPP TDL-C UMi and receiver 32 from the I2I Tx site-specific model. The KL Divergence of these PDPs is moderate, and the 3GPP model fails to capture all of the features of the site-specific model.

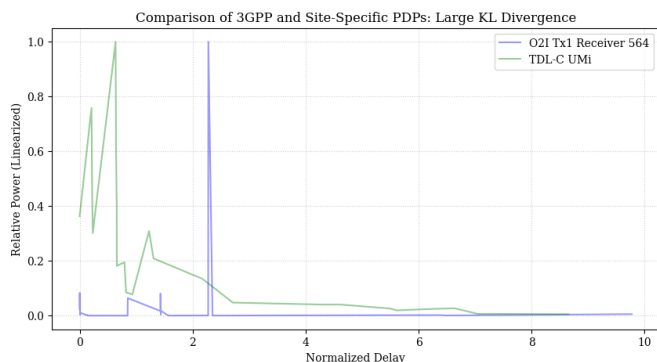


Fig. 7. A comparison of the normalized PDPs of 3GPP TDL-C UMi and receiver 564 from the O2I Tx1 site-specific model. The KL Divergence of these PDPs is large, and the 3GPP model does not reflect the main features of the site-specific model.

analogous PDP for the TDL-C model, and the difference between the PDPs is stark. Other receivers in both scenarios have substantial differences with some or all of the models.

Figure 6 illustrates an example of where a 3GPP model captures some, but not all, of the features of a site-specific model. Receiver 32 from the I2I site-specific model has a spike not reflected in TDL-A, resulting in a KL divergence value $D_{KL} = 1.16$.

There are also instances where the 3GPP models are reasonable estimates of the normalized site-specific models. The second O2I scenario, seen in Table V, is, in many cases, quite similar to the 3GPP models. The similarities between the PDPs TDL-C and receiver 484 are seen in Figure 5, illustrating a scenario where 3GPP models are still capturing the primary features of the site-specific scenario.

IV. CONCLUSION

This study compared the PDP characteristics of 3GPP TR 38.901 TDL models with the Wireless InSite deterministic ray-tracing simulations in dense urban O2I and I2I environments. Results demonstrate that while 3GPP TDL models exhibit longer overall delay spreads and statistical tails, site-specific models better preserve late-arriving multipath energy and deterministic structures, such as irregular power spikes, that standardized models often smooth or omit. KL divergence analysis reveals significant structural discrepancies, particularly in cases where 3GPP abstractions fail to capture primary geometry-driven features. We conclude that while 3GPP TDL models are suitable for large-scale system evaluation, deterministic or hybrid geometry-aware modeling is essential for site-specific physical-layer design, cyclic prefix dimensioning, and assessing inter-symbol interference sensitivity.

REFERENCES

- [1] 3GPP, "Study on channel model for frequencies from 0.5 to 100 GHz," 3rd Generation Partnership Project (3GPP), Technical Report (TR) 38.901, 4 2026, release 19. [Online]. Available: https://www.3gpp.org/ftp/Specs/archive/38_series/38.901/
- [2] P. Kyösti, J. Meinilä, L. Hentilä, X. Zhao, T. Jämsä, M. Narandzic, M. Milojević, A. Hong, J. Ylitalo, V.-M. Holappa, M. Alatossava, R. J. C. Bultitude, Y. Jong, and T. Rautiainen, "WINNER II Channel Models," IST-4-027756 WINNER II D1.1.2 V1.2, Technical Report, Feb. 2008. [Online]. Available: https://www.researchgate.net/publication/234055761_WINNER_II_channel_models
- [3] L. Liu, C. Oestges, J. Poutanen, K. Haneda, P. Vainikainen, F. Quitin, F. Tufvesson, and P. De Doncker, "The COST 2100 MIMO Channel Model," *IEEE Wireless Communications*, vol. 19, no. 6, pp. 92–99, 2012.
- [4] S. Y. Seidel and T. S. Rappaport, "A Ray Tracing Technique to Predict Path Loss and Delay Spread Inside Buildings," in *Proc. IEEE Global Telecommunications Conference (GLOBECOM)*, vol. 2, Orlando, FL, USA, Dec. 1992, pp. 649–653.
- [5] K. R. Schaubach, N. J. Davis, and T. S. Rappaport, "A Ray Tracing Method for Predicting Path Loss and Delay Spread in Microcellular Environments," in *Proc. IEEE 42nd Vehicular Technology Conference (VTC)*, vol. 2, Denver, CO, USA, May 1992, pp. 932–935.
- [6] A. Zhou, J. Huang, J. Sun, Q. Zhu, C.-X. Wang, and Y. Yang, "60 GHz Channel Measurements and Ray Tracing Modeling in an Indoor Environment," in *Proc. 9th International Conference on Wireless Communications and Signal Processing (WCSP)*, Nanjing, China, Oct. 2017, pp. 1–6.
- [7] Remcom, Inc., "Wireless InSite: 3D Wireless Prediction Software," 2026, [Online]. Accessed: May 8, 2026. [Online]. Available: <https://www.remcom.com/wireless-insite-propagation-software>

- [8] C. Phillips, D. Sicker, and D. Grunwald, "Bounding the Practical Error of Path Loss Models," *International Journal of Antennas and Propagation*, vol. 2012, no. 1, p. 754158, 2012. [Online]. Available: <https://onlinelibrary.wiley.com/doi/abs/10.1155/2012/754158>
- [9] S. Kullback and R. A. Leibler, "On information and sufficiency," *The annals of mathematical statistics*, vol. 22, no. 1, pp. 79–86, 1951.
- [10] H. Kulhandjian and T. Melodia, "Modeling underwater acoustic channels in short-range shallow water environments," in *Proceedings of the 9th International Conference on Underwater Networks & Systems*, 2014, pp. 1–5.